Stem Cell–Derived Photoreceptor Transplants Differentially Integrate Into Mouse Models of Cone-Rod Dystrophy

Tiago Santos-Ferreira,[1] Manuela Völkner,[2] Oliver Borsch,[1] Jochen Haas,[1] Peter Cimalla,[3] Praveen Vasudevan,[1] Peter Carmeliet,[4] Denis Corbeil,[5] Stylianos Michalakis,[6] Edmund Koch,[3] Mike O. Karl,[1,2] and Marius Ader[1]

[1]Technische Universität Dresden, CRTD - Center for Regenerative Therapies Dresden, Dresden, Germany
[2]German Center for Neurodegenerative Diseases (DZNE), Dresden, Germany
[3]Technische Universität Dresden, Faculty of Medicine Carl Gustav Carus, Department of Anesthesiology and Intensive Care Medicine, Dresden, Germany
[4]Laboratory of Angiogenesis and Vascular Metabolism, VIB - Vesalius Research Center, University of Leuven, Department of Oncology, Leuven, Belgium
[5]Technische Universität Dresden, Biotechnology Center, Dresden, Germany
[6]Center for Integrated Protein Science Munich (CiPSM), Department of Pharmacy - Center for Drug Research, Ludwig-Maximilians-Universität München, Munich, Germany

Correspondence: Mike O. Karl, German Center for Neurodegenerative Diseases Dresden (DZNE), Arnoldstraße 18, 01307 Dresden, Germany; mike.karl@dzne.de.
Marius Ader, Technische Universität Dresden, Center for Regenerative Therapies Dresden, Fetscherstraße, 105, 01307 Dresden, Germany; marius.ader@crt-dresden.de.

TS-F and MV contributed equally to the work presented here and should therefore be regarded as equivalent authors.

Submitted: January 6, 2016
Accepted: May 22, 2016

Citation: Santos-Ferreira T, Völkner M, Borsch O, et al. Stem cell–derived photoreceptor transplants differentially integrate into mouse models of cone-rod dystrophy. *Invest Ophthalmol Vis Sci*. 2016;57:3509–3520. DOI:10.1167/iovs.16-19087

Purpose. Preclinical studies on photoreceptor transplantation provided evidence for restoration of visual function with pluripotent stem cells considered as a potential source for sufficient amounts of donor material. Adequate preclinical models representing retinal disease conditions of potential future patients are needed for translation research. Here we compared transplant integration in mouse models with mild (prominin1-deficient; Prom1$^{-/-}$) or severe (cone photoreceptor function loss 1/rhodopsin-deficient double-mutant; Cpfl1/Rho$^{-/-}$) cone-rod degeneration.

Methods. For photoreceptor transplant production, we combined the mouse embryonic stem cell retinal organoid system with rhodopsin-driven GFP cell labeling by recombinant adeno-associated virus (AAV). Organoid-derived photoreceptors were enriched by CD73-based magnetic-activated cell sorting (MACS) and transplanted subretinally into wild-type, Prom1$^{-/-}$ and Cpfl1/Rho$^{-/-}$ hosts. The survival, maturation, and synapse formation of donor cells was analyzed by immunohistochemistry.

Results. Retinal organoids yielded high photoreceptor numbers that were further MACS-enriched to 85% purity. Grafted photoreceptors survived in the subretinal space of all mouse models. Some cells integrated into wild-type as well as Prom1$^{-/-}$ mouse retinas and acquired a mature morphology, expressing rod and synaptic markers in close proximity to second-order neurons. In contrast, in the novel Cpfl1/Rho$^{-/-}$ model with complete photoreceptor degeneration, transplants remained confined to the subretinal space, expressed rod-specific but only reduced synaptic markers, and did not acquire mature morphology.

Conclusions. Comparison of photoreceptor grafts in preclinical models with incomplete or complete photoreceptor loss, showed differential transplant success with effective and impaired integration, respectively. Thus, Cpfl1/Rho$^{-/-}$ mice represent a potential benchmark model resembling patients with severe retinal degeneration to optimize photoreceptor replacement therapies.

Keywords: pluripotent stem cells, retina, mouse, transplantation, neurodegeneration

Vision is one of the most important senses for humans, and its impairment or complete absence significantly hampers daily life of affected patients. One of the major causes for blindness in industrialized countries is the loss of photoreceptors, as in age-related macular degeneration (AMD), retinitis pigmentosa (RP), or cone-rod dystrophies (CRD). So far, there is no definite cure available to preserve or restore vision.[1] Several therapies are being developed with first treatments currently evaluated in clinical trials; however, particularly neuroprotective or gene therapeutic approaches require the presence of endogenous photoreceptors.[2–6] In contrast, cell replacement approaches represent a potential therapy for retinal dystrophies characterized by photoreceptor cell loss.

Several studies demonstrated the feasibility of photoreceptor replacement therapy using primary rod photoreceptors[7–10] isolated from young postnatal mouse retinas, enriched by cell surface markers[9,11–13] or fluorescent proteins[11] and grafted into the subretinal space of adult wild-type or photoreceptor-degenerating mice. Grafted photoreceptors integrated into the retinal host tissue, acquired mature photoreceptor mor-

Investigative Ophthalmology & Visual Science

phology, expressed rod-specific markers, and formed synapses to corresponding second-order neurons.[7–10,14] In fact, rod photoreceptor transplantation allowed the restoration of night vision in mouse models of stationary night blindness.[12,15] Furthermore, transplantation of cone-like photoreceptors into a mouse model of cone degeneration restored responses in retinal ganglion cells in daylight conditions.[16] Thus, photoreceptor transplantation in animal models represents an excellent approach for preclinical proof-of-principle studies.

The use of primary photoreceptors for clinical application would raise multiple logistical and ethical concerns, whereas other donor cell sources, such as pluripotent stem cells (embryonic stem cells [ES] and induced pluripotent stem cells [iPS]) avoid these concerns once they can be generated in sufficient numbers at clinical grade. In recent years, the generation of retinal cells in two-dimensional (2D) and stratified retinal tissue in a three-dimensional (3D) culture system from mouse (m) ES[17] and human (h) ES/hiPS[18–22] were accomplished, which became suitable tools to generate rod photoreceptors for transplantation studies.[23–25]

To develop a clinical grade in vitro source of transplantable photoreceptors and assessing transplant success based on functional recovery, adequate mouse models have to be established that represent retinal degenerative conditions found in patients who might benefit from future transplantation approaches. Thus, mouse models of retinal diseases with defects resulting in complete (i.e., combined cone and rod) photoreceptor loss represent a proper standard to evaluate transplant integration. Lack of endogenous photoreceptors makes the host retina a hostile environment and unsuitable for other treatment approaches, such as gene therapy or neuroprotection, whereas such condition represents the target for cell replacement therapies with the aim to replace lost photoreceptors. Indeed, ES-derived photoreceptor transplant efficiencies in various disease types and stages (i.e., in presence or particularly absence of endogenous photoreceptors) remain incompletely understood.[23,25]

In this study, we evaluated the combined application of organoid retinogenesis and magnetic-activated cell sorting (MACS) technology to generate and enrich high quantities of mES-derived rod photoreceptors as a potential future strategy for applicable photoreceptor transplantation. We assessed the quality of the photoreceptor transplant product by comparing donor cell integration to previous data on primary photoreceptors. We established a double-mutant mouse model with combined rod and cone functional deficit, which results in complete photoreceptor degeneration. Comparative photoreceptor transplantation studies in mouse models with either incomplete or complete photoreceptor loss suggest differential therapy success, with effective and impaired integration, respectively.

Methods

Animals

Adult age-matched (7–12 weeks) wild-type (C57BL/6J), Prominin-1 knock-out (Prom1$^{-/-}$),[26] and cone photoreceptor function loss 1 (Cpfl1)[27] crossed to rhodopsin knock-out mice (Rho$^{-/-}$),[28] tg(Cpfl1;Rho$^{-/-}$), were used as hosts for transplantation. All animal experiments were approved by the ethics committee of the Technische Universität Dresden and the Landesdirektion Dresden (approval no. 24-9168.11-1/2013-23) and performed in accordance with the regulations of the European Union, German laws (Tierschutzgesetz), the ARVO Statement for the Use of Animals in Ophthalmic and Vision Research, as well as the National Institutes of Health Guide for the care and use of laboratory work.

Mouse ES–Derived Retinal Organoid Differentiation and Adeno-Associated Virus Transduction

Wild-type E14TG2a (MMRRC, University of California Davis, Davis, CA, USA) mES were cultured on 10-cm tissue culture plates (BD Falcon, Heidelberg, Germany) in mES medium supplemented with 10^3 U/mL LIF and 1 μM PD0325901. Cells were passaged every 2 to 3 days (70% confluence) using TrypLE Express (Invitrogen, Schwerte, Germany) and reseeded at 0.5 to 1.0 × 10^6 cells per plate. Medium was changed daily. To generate aggregates, dissociated mES were seeded at 3000 cells per 100 μL per 96-well (U-bottom, low adhesion; Lipidure Coat, NOF, White Plains, NY, USA) in retinal differentiation medium (RDM); 2% Matrigel (growth factor reduced; BD Biosciences, Heidelberg, Germany) was added on day (D) 1, defining the day the differentiation protocol started as D0. Organoids were transferred to bacterial-grade Petri dishes (Greiner Bio-One, Frickenhausen, Germany) on D9, and cultured (37°C, 5% CO_2, 20% O_2,) in retinal maturation medium (RMM). Fifty percent of medium was changed every 2 to 3 days including EC23 (0.3 μM; Tocris, Avonmouth, Bristol, UK) from D14. Organoids were transduced with AAV2/8YF Rho–green fluorescent protein (GFP)[29] (1 × 10^{10} vector genomes [vg]/organoid) from D20 to 22 followed by complete media change. The number of biological replicates was defined as experiments started from separate mES preparations (N) and the technical replicates as the number of individual organoids analyzed (n). Adeno-associated virus vectors were produced and purified as previously described.[29] Genomic titers were determined as previously described[30,31] with one of the following primer pair combinations: ITR2F, 5′-GGA ACC CCT AGT GAT GGA GTT-3′ and ITRR, 5′-CGG CCT CAG TGA GCG A-3′ or GFPF, 5′-TTC TCG TTG GGG TCT TTG CTC AG-3′ and GFPR, 5′-CGA CCA CTA CCA GCA GAA CAC-3′. For more details on media composition, AAV production, retinal organoid immunohistochemistry, and RT-PCR see Supplementary Methods.

Magnetic-Activated Cell Sorting Enrichment and Transplantation of mES-Derived Rod Photoreceptors

Mouse ES–derived rods were enriched using an adapted protocol of MACS methodology for primary rods.[9,13] Briefly, organoids on D26 were enzymatically digested to a single cell suspension using Papain dissociation kit (Worthington, Lakewood, NJ, USA) and resuspended in MACS buffer. Cell suspensions were incubated (5 minutes) with CD73 antibody (BD Pharmingen, Heidelberg, Germany) followed by 15 minutes with magnetic bead-conjugated secondary antibodies (Miltenyi, Bergisch Gladbach, Germany). The CD73-negative and CD73-positive cell fractions were collected following MACS and the percentages of CD73-positive cells in un-, positive-, and negative-sorted cell fractions were determined by flow cytometry.

To assess the transduction potential of residual AAV virus in MACS-purified photoreceptors, separate D20 organoids were incubated with supernatant of freshly MACS-purified CD73-positive cells (AAV2/8YF Rho-GFP transduction on D20, MACS on D26) and the organoids were analyzed for GFP expression on D26. Additionally, AAV genomic titters at D21 and before/after MACS purification were determined.

Freshly enriched photoreceptors were transplanted into the subretinal space of adult mice following procedures described in detail elsewhere.[13,16] A total of 1 μL MACS buffer containing 2×10^5 mES-derived rods was transplanted subretinally in the nasal region of the eye. Experimental animals were killed 3 to 4 weeks after transplantation.

Tissue Processing, Immunohistochemistry, and Analysis

Experimental animals were euthanized and eyes were enucleated and fixed with 2% to 4% paraformaldehyde (Sigma, Munich, Germany) for 20 to 60 minutes and processed for cryosectioning; 20-μm retinal sections were treated with 0.3% Triton X-100, 5% donkey serum, and 1% BSA (Sigma). Retinal sections were immunostained with primary antibodies (Supplementary Table S1), followed by fluorophore-conjugated secondary antibodies combined with nuclear stain 4′, 6-diamidino-2-phenylindole (DAPI; Sigma).

Stained sections were imaged using an Apotome ImagerZ1 and analyzed with Axiovision Software (Zeiss, Oberkochen, Germany), Fiji (National Institutes of Health, Bethesda, MD, USA), and Illustrator CS6 (Adobe Systems, Inc., San Jose, CA, USA). Integrated photoreceptors were quantified as described elsewhere.[16] Briefly, GFP-positive cell bodies that were located in the outer nuclear layer (ONL) and contained an inner segment, or synaptic terminal, or both, and neurites were considered as integrated photoreceptors. Data were plotted using Prism and statistical significance was calculated using unpaired, 2-tailed Student's *t*-test and displayed as ** $P < 0.01$, *** $P < 0.005$.

Results

Generation of Transplantable Rho-GFP Labeled Rod Photoreceptors

We modified a previously published protocol (see Methods[23]) to achieve efficient differentiation of mES-derived retinal organoids containing high amounts of rod photoreceptors for transplantation (Fig. 1; Supplementary Fig. S1). The mES-derived organoids grew in size (Fig. 1B) and developed potential eyefield areas by D7 based on immunostaining for eyefield transcription factor Rx (82% ± 12%, $N = 7$, $n \geq 10$ aggregates [*n*] per biological replicate [*N*], Supplementary Fig. S1A). Immunostaining analysis showed that organoid epithelia started to develop a layered structure with large numbers of Crx^+ photoreceptor precursors consistently detected by D16. Photoreceptors were localized toward the apical side (organoid inside), whereas amacrines ($HuCD^+$) and ganglion cells ($HuCD^+$, $Brn3^+$, $Rbfox3^+$) formed a layer at the basal side (Supplementary Figs. S1B, S1C). At this stage, many retinal progenitor cells were still present (Rx^+, $Vsx2^+$), which underwent mitosis (phospho-histone H3, $PHH3^+$) apically (Supplementary Figs. S1A1, S1A2). By D24, rod photoreceptors expressed more mature photoreceptor markers, like recoverin and rhodopsin (Figs. 1C1, 1D), and the formation of a stratified retina became prominent (Supplementary Figs. S1E, S1F). Bipolars ($Vsx2^+$), horizontals ($Calb1^+$), and Müller glia (glutamine $synthetase^+$) were located in an intermediate layer (Supplementary Fig. S1G). Expression analysis by RT-PCR of Nrl, Irbp, Cnga1, Pias3, Pde6b, Rxrg, and recoverin (Rcvn) on D26 further indicate photoreceptor genesis in mES-derived organoids.

Usually several smaller retinal domains were observed in each aggregate, which compose the major part of the aggregate circumference (1251 ± 312 μm $recoverin^+$ circumferential length, $n = 10$; Figs. 1C, 1D). However, although the photoreceptor layer was well developed, the inner retinal layers are considerably thinner (Supplementary Figs. S1C, S1E, S1F) and organoids thus are naturally enriched for rods, as previously reported.[23]

To label rods for transplantation experiments, we transduced organoids at D20 with AAV vectors carrying a rhodopsin-driven GFP cassette (AAV Rho-GFP) (Figs. 1A, 1E; Supplementary Figs. S2A–C). Adeno-associated virus–based gene transfer has been used for gene delivery and gene therapy to the retina, including photoreceptors.[6] Green fluorescent protein expression was detected 4 to 5 days after transduction in the retinal epithelial layer of all organoids incubated with AAV (Figs. 1C, 1E; Supplementary Fig. S1D). Immunostaining of D24 organoids showed that GFP^+ cells coexpress the pan-photoreceptor marker recoverin (Fig. 1C) and rod-specific marker rhodopsin (Supplementary Fig. S1D), confirming rod-specific GFP expression of the Rho-GFP construct. Many $recoverin^+$ and $rhodopsin^+$ cells also expressed GFP, suggesting a sufficient viral transduction efficiency.

Previously, carryover of AAV particles resulting in transduction and thus unwanted reporter expression of host photoreceptors has been observed after transplantation of AAV-GFP labeled donor photoreceptors.[23] To test for the presence of potentially contaminating AAV particles in the supernatant of retinal organoid cultures and photoreceptor suspensions for transplantation, the amount of residual vector genomes was quantified using quantitative PCR. The residual AAV genomic titer already in the supernatant dropped by more than 3 log units 24 hours after transduction ($4.3–6.2*10^7$ vg/μL), and more than 6 log units ($3.4–6.2*10^4$ vg/μL) at D26 before and after MACS, respectively. Such low titers in the range of 10^4 vg/μL cannot result in any significant GFP expression after retinal injection, as a minimum of 10^7 vg/μL is estimated to result in significant numbers of transduced photoreceptors[15] (our own unpublished observations, 2015). Indeed, in retinal organoids transduced with supernatant from D26 CD73-MACS enriched organoid-derived photoreceptors with an AAV titer of $4.1–6.4*10^4$ vg/μL, no GFP labeled cells were detectable (Supplementary Figs. S2D, S2E; $n = 10$), suggesting a negligible potential for transduction of endogenous photoreceptors by remaining AAV particles after transplantation. These results confirm that the GFP fluorescence observed in our transplantation experiments derived from donor photoreceptors.

CD73-Based MACS Enrichment of mES-Derived Rod Photoreceptors and Grafting Into the Wild-Type Mouse Retina

Retinal organoids contain heterogeneous cell populations; thus, their direct use for photoreceptor replacement studies might not result in an optimal therapeutic outcome due to risks of tumor formation, cell contamination, and/or acute immune responses.[32–34] To reduce such complications, we pursued the isolation and enrichment of photoreceptors. Hence, we applied our established protocol for enrichment of primary rod photoreceptors by CD73-based MACS to mES-derived photoreceptors (Figs. 1F, 1G). Gene expression analysis by RT-PCR at D12 and D26 support retinogenesis in the organoid system, as transcription factors Pax6, Lhx2, Otx2, Sox9, and Vsx2 with major functions in retinal development are expressed. Our analysis revealed that CD73 (Nt5e) gene expression starts along with the photoreceptor transcription factor Crx at D12 and both were prominently detected at D26, but not in pluripotent marker (Oct4 and Nanog) positive mES (Supplementary Fig. S3).

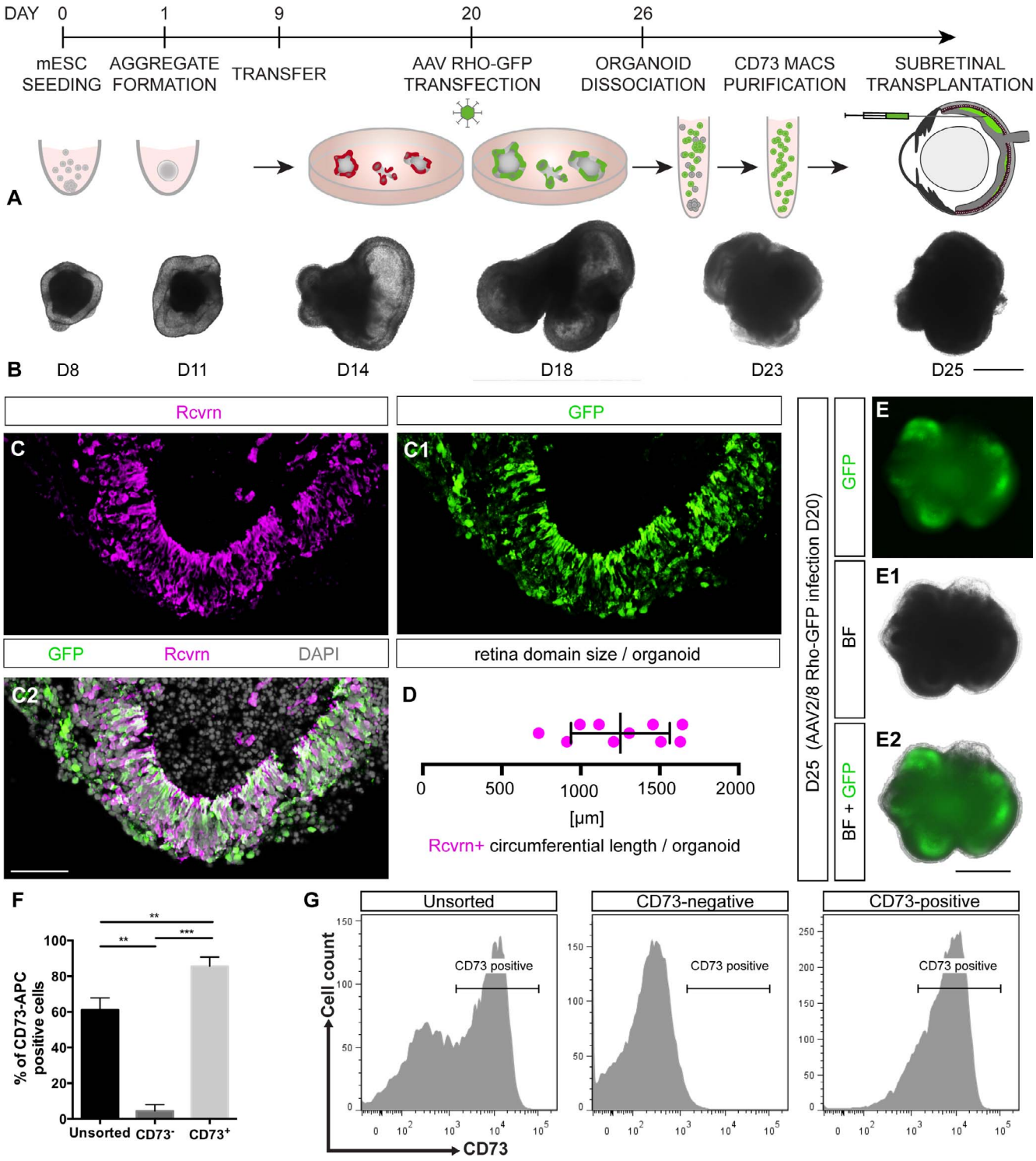

Figure 1. Generation, viral transduction, and enrichment of rods derived from retina organoids. (**A**) Schematic overview of the retinal differentiation and rod photoreceptor transplantation procedure. Mouse ES were differentiated to retina organoids, containing high numbers of rod photoreceptors. Rods were labeled by transduction with adeno-associated virus (AAV) Rho-GFP at D20 of the differentiation protocol. For transplantation, organoids were dissociated on D26, rods were enriched by MACS using CD73 antibody and transplanted into the subretinal space of adult mouse eyes. (**B**) Representative phase-contrast images of mES-derived retinal organoids at different stages of differentiation. (**C**) AAV Rho-GFP–labeled cells (*green*; C1) coexpress the pan-photoreceptor marker recoverin (Rcvrn, *red*; C, C2 is an overlay of C and C1) at D26. (**D**) Quantification of the size of the retina domains in organoids positive for recoverin (Rcvrn). (**E**) D25 retina organoids transduced with AAV Rho-GFP at D20 show GFP (*green*; E) expression in large parts of the organoid (E1, bright field [BF]), especially along the outer epithelial layer (E2; overlay of E and E1). (**F**) Quantitative analysis of CD73 expressing cells by flow cytometry before (unsorted) and after CD73-based MAC sorting of mES-derived rods isolated on D26 of organoidogenesis. Graph shows that dissociated unsorted organoids contained approximately 61% $CD73^+$ cells, whereas CD73-based MAC sorting significantly enabled enrichment to approximately 85% $CD73^+$ cells ($n = 3$). The $CD73^-$ fraction only contained a small fraction of $CD73^+$ cells (~4%). (**G**) Representative CD73 flow cytometry analysis plots. $^{**}P < 0.01$, $^{***}P < 0.005$ paired Student's *t*-test. n = biological replicates. *Scale bars*: 500 µm (**B**, **C**) and 50 µm (**E**).

Investigative Ophthalmology & Visual Science

A single cell suspension of 15 to 20 pooled D26 organoids was sorted by CD73-based MACS. Unsorted, $CD73^+$ and $CD73^-$ fractions were reanalyzed by flow cytometry using APC-conjugated secondary antibody (Figs. 1F, 1G). Reanalysis for $CD73^+$ cells showed that the unsorted fraction contained 61% ± 4% SEM, the $CD73^+$ fraction contained 86% ± 3% SEM, and the $CD73^-$ fraction contained 4% ± 2% SEM (Fig. 1F), indicating that the MACS technology can be used to enrich retinal organoid-derived rod photoreceptors.

Next, we transplanted CD73-enriched and rAAV2/8 Rho-GFP transduced photoreceptors into the subretinal space of wild-type mice. Donor cells survived in the subretinal space at least up to 4 weeks and a fraction of GFP^+ cells were located within the ONL (Supplementary Fig. S4). Integrated rods acquired mature photoreceptor morphology, with apically located inner and outer segments (arrow, Supplementary Fig. S4B) and cell bodies located in the ONL (arrowhead, Supplementary Fig. S4B). GFP^+ processes indicate the presence of synaptic terminals of integrated photoreceptors in the outer plexiform layer (Supplementary Figs. S4C, S5).

Grafted photoreceptors expressed the pan-photoreceptor marker recoverin (Supplementary Figs. S4B, SB1, SB3) and the rod-specific photo-transduction markers rhodopsin (Supplementary Figs. S4B, SB1, SB4), arrestin-1 (arrowheads, Supplementary Figs. S4C, SC1, SC3), and transducin (Supplementary Figs. S4D, SD1, SD3). Further, analysis of the established synaptic contacts showed synaptic spherules of integrated photoreceptors in close proximity to the dendritic tips of host rod bipolars ($PKCa^+$) and horizontals ($calbindin^+$) (Supplementary Fig. S5A). Three-dimensional reconstruction highlights the close proximity between GFP^+ axonal terminals of integrated cells and the dendritic tips of the host's second-order neurons (Supplementary Video S1). In addition to properly connected synaptic spherules, the presence of synaptic machinery components is essential in visual function to transmit the chemical signal from donor photoreceptors to second-order neurons. We observed the presence of several presynaptic markers (synaptophysin,[35] PSD95,[36] and RIBEYE[37]) and a synapse adaptor protein (pikachurin[38]) in integrated photoreceptors in a correct pattern resembling wild-type rod photoreceptor synapses (Supplementary Figs. S5B, S5C, S5D).

The integration efficiency of transplanted ES-derived photoreceptors into the ONL of wild-type hosts (1864 ± 245 GFP^+ cells/retina) was similar to the numbers reported in previous studies using primary photoreceptors isolated from young postnatal mice.[7–9]

Transplantation of mES-Derived Rods Into Retinal Degeneration Mouse Models

Enriched donor rods were transplanted into the subretinal space of two different adult mouse models of photoreceptor degeneration (7–12 weeks old). $Prom1^{-/-}$ mice show a slow cone-rod degeneration and gradual function loss with virtually complete photoreceptor cell loss 7 months after birth.[26,39] Four weeks after transplantation, grafted rods survived in the subretinal space and a fraction integrated into the ONL of $Prom1^{-/-}$ retinas, although photoreceptor degeneration was already progressed as indicated by the reduced ONL thickness (Fig. 2A) compared with wild-type retina (Fig. 2B). Grafted GFP^+ cells integrated in the ONL, acquired mature rod photoreceptor morphology with an inner and outer segment, a synaptic spherule, and a cell body located in the ONL (Fig. 3A). All integrated donor rods expressed proteins of the photo-transduction cascade (rhodopsin, recoverin, arrestin-1, and rod transducin; Figs. 3A–C). The axonal terminals of integrated donor cells were in close proximity to rod bipolars and horizontals (Fig. 4A, arrowheads and arrow, respectively) and their synaptic terminals expressed synaptophysin, PSD95, pikachurin, and RIBEYE (Figs. 4B–D). These results are coherent with our transplantation data in wild-type hosts (see above). Notably, transplanted donor cells integrated into the ONL with similar efficiencies (Fig. 4E) in wild-type (1864 ± 245 GFP^+ cells/retina) and $Prom1^{-/-}$ (1129 ± 337 GFP^+ cells/retina) retinas.

Most of the photoreceptor transplantation studies performed so far used mouse models, like the $Prom1^{-/-}$, in the early stages of yet incomplete retinal degeneration.[10,15,23,33,34] However, little is known about the behavior of donor photoreceptors in more severely degenerated retinas.[12,40] Hence, we established the tg(Cpfl1;$Rho^{-/-}$) mouse model, by crossing the cone photoreceptor function loss 1 (Cpfl1)[27] with rhodopsin knock-out ($Rho^{-/-}$)[28] mice resulting in mice with no functional photoreceptors starting from eye opening with the ONL rapidly degenerating to about one row of cell bodies within 10 to 12 weeks (Fig. 2).

Following transplantation, photoreceptors survived in the subretinal space of tg(Cpfl1;$Rho^{-/-}$) mice and expressed all photo-transduction markers analyzed, including rhodopsin, recoverin, arrestin-1, and rod transducin (Fig. 5). Transplanted donor rods formed subretinal clusters and did not acquire a polarized morphology as observed in $Prom1^{-/-}$ or wild-type recipients following integration into the ONL. Grafted rods remained in the subretinal space as a flat thin layer apposing host bipolars (Figs. 5A, 5B, 6). Analysis of retinal function was performed using ERG measurements, but no functional recovery was detected in eyes with rod transplants compared with control animals (data not shown).

To elucidate whether the absence of functional rescue might be due to incomplete graft integration, we analyzed contacts of donor cells with the host residual neuronal circuitry. Transplanted photoreceptor cells were located in close proximity to rod bipolars and horizontals, but dendrites from bipolars and horizontals did not reestablish their arborization following transplantation (Fig. 6A) when compared with their wild-type counterpart (Supplementary Fig. S5A). Moreover, grafted mES-derived rods showed reduced expression of the synaptic markers synaptophysin and PSD95, whereas pikachurin and RIBEYE were barely detectable in a few transplanted cells (Figs. 6B–D).

Discussion

Photoreceptor replacement by cell transplantation represents a promising therapeutic strategy for incurable retinal degenerative diseases. In this study, we developed a workflow for the production of virally GFP-labeled transplantable donor rod photoreceptors from mouse retinal organoids. We demonstrate that mES-derived organoids not only yield high amounts of rod photoreceptors but also that they can be enriched by cell surface marker–based MACS. This results in sufficient amounts of transplantation-competent photoreceptors for cell replacement approaches in preclinical mouse models of photoreceptor loss.

Recent advances in the generation of photoreceptors from mouse and human pluripotent stem cells in vitro[17,18,41–43] built the basis for the development of potential cell replacement therapies in the retina. Indeed, first studies provided evidence for successful generation and transplantation of mouse ES-derived photoreceptors in preclinical models of retinal degeneration.[23,25] However, further optimization steps will be required to develop photoreceptor replacement strategies toward clinical application.

The use of donor cells for clinical use requires certain ethical and safety considerations. Particularly when using

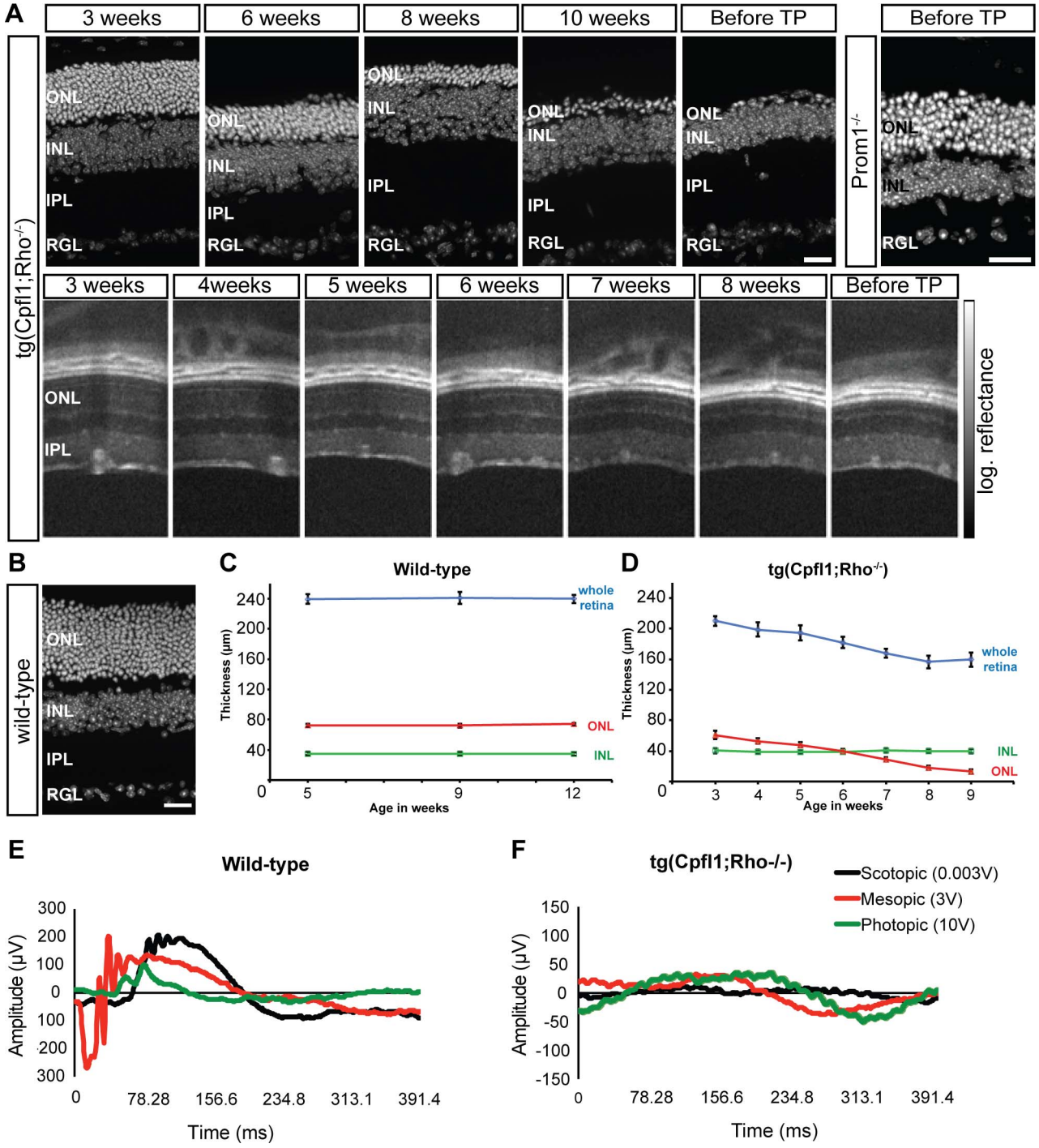

Figure 2. Characterization of tg(Cpfl1;Rho$^{-/-}$) transgenic mice. (**A**) Cross-sectional images of tg(Cpfl1;Rho$^{-/-}$) retinas using immunohistochemistry and optic coherence tomography (OCT) show the retinal degeneration process resulting in complete loss of the ONL at 10 weeks. Histologic characterization of both recipient degeneration models, tg(Cpfl1,Rho$^{-/-}$) and Prom1$^{-/-}$, before transplantation (TP) and comparison with wild-type controls (**B**). (**C**, **D**) Quantification of retinal thickness in wild-type and tg(Cpfl1;Rho$^{-/-}$) mice over a period of 12 weeks. The tg(Cpfl1;Rho$^{-/-}$) mice show a significant decrease in the thickness of the ONL between 3 and 9 weeks when compared with age-matched wild-types, while the inner nuclear layer (INL) remains constant over this period. (**E**, **F**) Representative ERG measurements comparing 12-week-old wild-type (**E**) and tg(Cpfl1;Rho$^{-/-}$) (**F**) mice show flattened ERG curves in scotopic, mesopic and photopic conditions for the retinal degeneration model. *Scale bars*: (**A**), (**B**): 20 µm. IPL, inner plexiform layer; RGL, retinal ganglion layer.

pluripotent stem cell–derived products, the danger of initiating tumor growth has to be ruled out.[33] Besides proper differentiation into the target cell types, enrichment steps for their purification before transplantation might be necessary. Therefore, we studied the use of the cell surface marker CD73 as a potential selector for transplantable rods generated in mES-derived retinal organoids.[9,11,44] Indeed, we found comparable numbers of CD73^{+} cells (~60%) in retinal organoids at D26 as in mouse retinas in vivo at postnatal day 4 (P4)[9] that could be further enriched by MACS to 85%. Thus, the use of a single cell

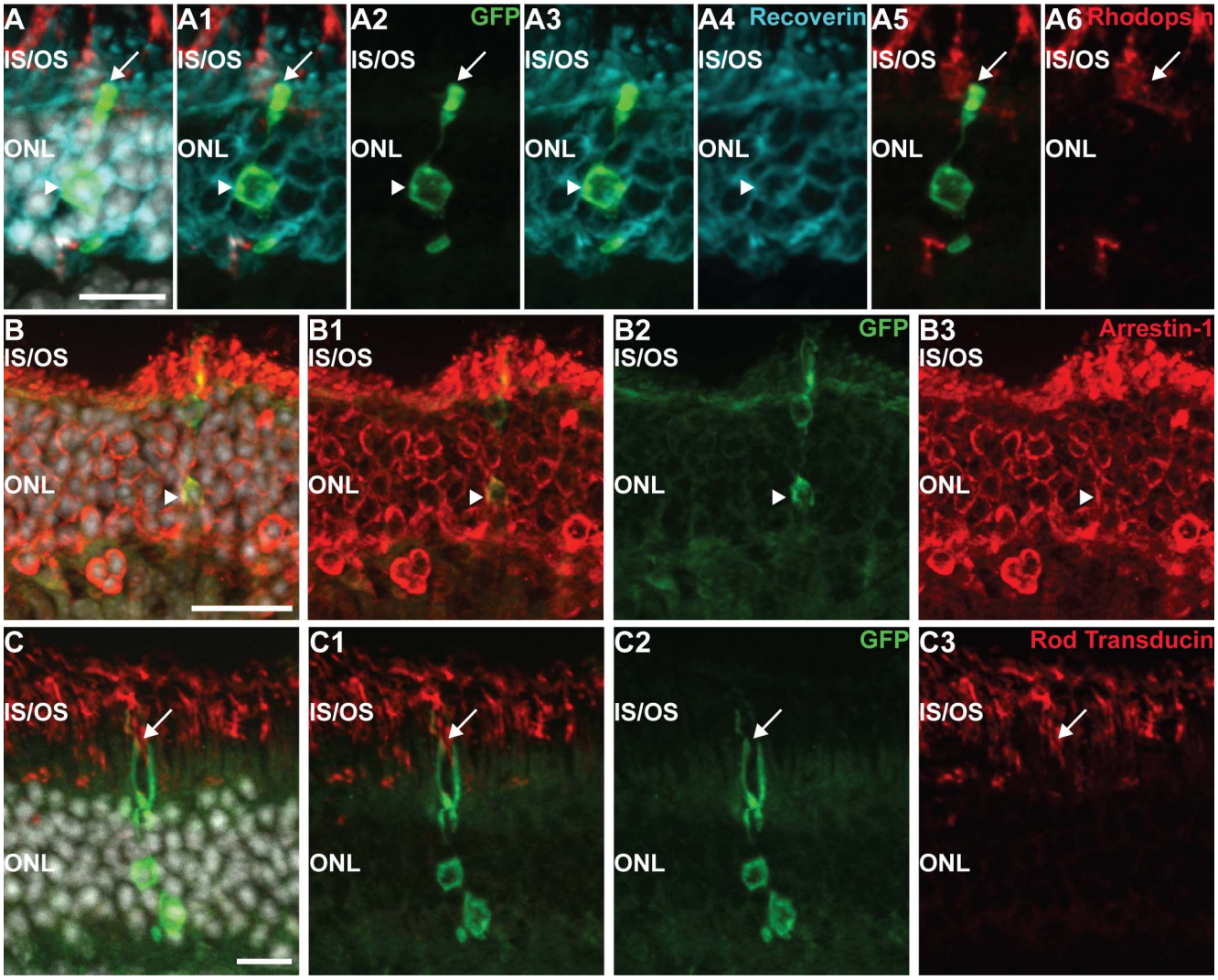

FIGURE 3. Integration of transplanted mES-derived rods into the prominin1 knock-out (Prom1$^{-/-}$) mouse retina. Transplanted mES-derived rods acquire mature rod photoreceptor morphology and express the photo-transduction markers rhodopsin (*arrow* in **A**, **A1**, **A5**, **A6**; *red*), recoverin (*arrowhead* in **A**, **A1**, **A3**, **A4**; *cyan*), arrestin-1 (*arrowhead* in **B**, **B1**, **B3**; *red*) and rod transducin (*arrow* in **C**, **C1**, **C3**; *red*) upon transplantation into adult Prom1$^{-/-}$ mice. Nuclei were counterstained with DAPI (*gray*). *Scale bars*: (**A**) and (**C**): 10 μm; (**B**): 20 μm. IS/OS, inner segment/outer segment; OPL, outer plexiform layer.

surface marker to enrich rod photoreceptors from retinal organoids might be sufficient to ensure safety during transplantations, as we did not observe tumor formation within the course of our studies. Nevertheless, long-term studies have to be conducted to assess safety of this approach and, if necessary, to further optimize the sorting procedure using a panel of markers that allow the selection of a specific subpopulation with optimal features for transplantation. Lakowski and colleagues[45] recently identified a combination of five cell surface markers that allowed the enrichment of transplantation-competent mES-derived rod precursors by fluorescence-activated cell sorting. Enrichment of transplantable donor cells for clinical use by flow cytometry has only been established in few locations due to challenges in applying to Good Manufacturing Practices (GMP) conditions, whereas MACS enrichment has been extensively used in clinical trials with, for example, hematopoietic stem cells,[46–48] and therefore might be also applicable in the generation of clinical grade human photoreceptors for cell replacement applications in patients. Here, we provide evidence that MACS-based enrichment of photoreceptors produced in the organoid system is a proficient method for effective cell replacement therapy in preclinical mouse models and healthy wild-type mice.

Similar to primary rod photoreceptors,[7,9,15,40] mES-derived rods showed robust survival following transplantation into the subretinal space of adult wild-type mice. Furthermore, full maturation of in vitro generated rods was observed in vivo, particularly when donor cells integrated into the host ONL demonstrating the potential of mES-derived rod photoreceptors for cell replacement approaches. Besides full maturation of grafted rods, including expression of proteins of the photo-transduction machinery, we observed the expression of several synaptic markers in donor-derived synaptic spherules in close proximity to rod bipolar and horizontal cells, suggesting integration into the retinal circuitry of wild-type hosts.

There are notable differences on rod transplantation in the two mouse models of retinal degeneration used in this study. Our results in the slowly degenerating Prom1$^{-/-}$ mouse are in line with previous reports that showed the feasibility of grafted photoreceptor integration in several retinal disease mouse models with remaining ONL,[10,15] with efficient rod graft integration and survival up to 4 weeks, resembling our

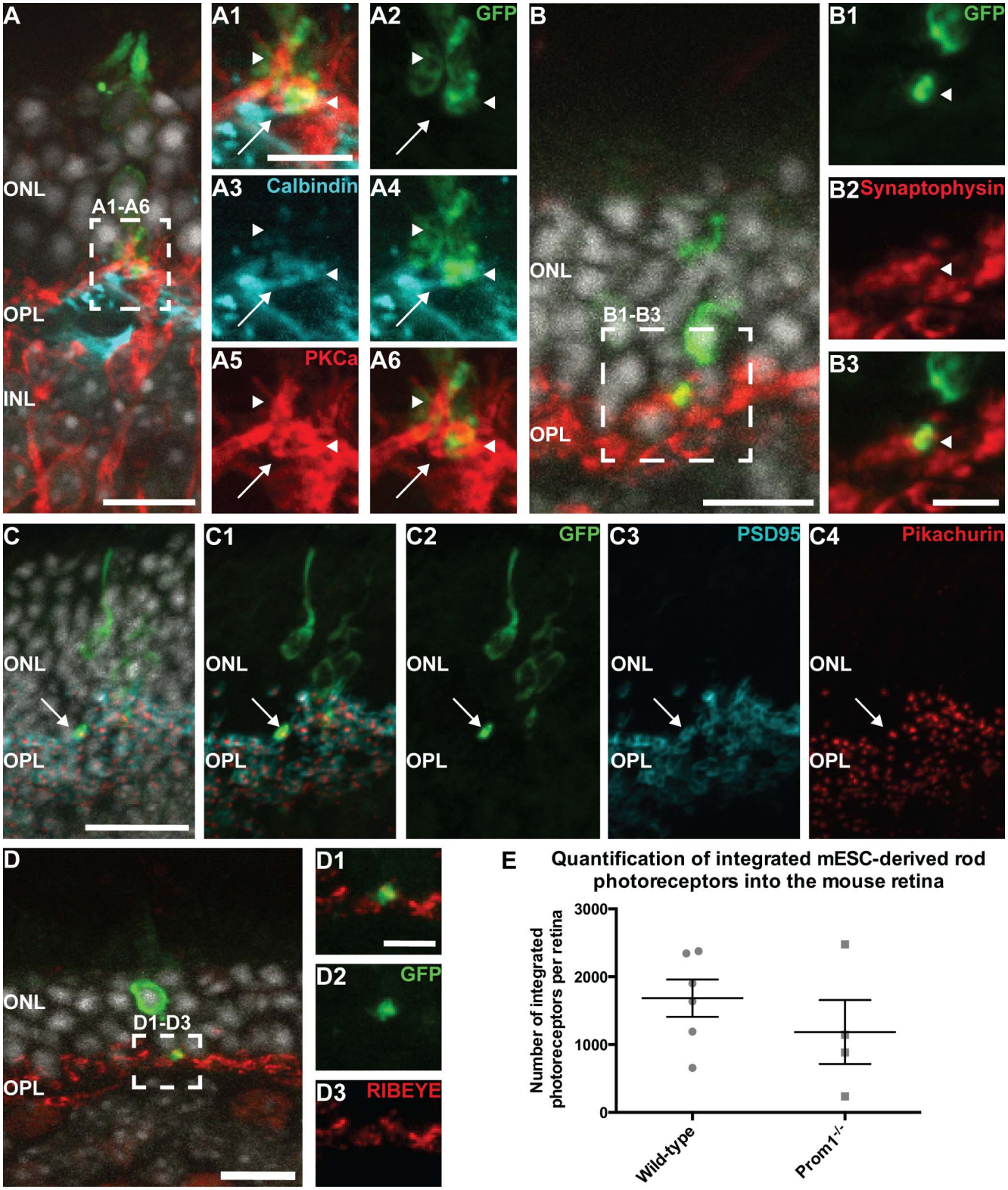

Figure 4. Synapse formation of mES-derived rods transplanted into Prom1$^{-/-}$ mice. (**A**) Donor rods (*green*, GFP) establish axonal terminals in close proximity to rod-bipolar (*arrowhead* in (**A1–A6**; *red*) and horizontal (*arrow* in **A1–A6**; *cyan*) cells following transplantation into the prom1$^{-/-}$ retina. (**B–D**) Integrated mES-derived rods express the synaptic markers synaptophysin (*arrowhead* in **B1–B3**), PSD95 (*arrow* in **C**, **C1**, and **C4**), pikachurin (*arrow* in **C**, **C1**, **C4**) and RIBEYE (**D**, **D1**, **D3**). (**E**) Donor rods integrated with similar efficiencies into wild-type and Prom1$^{-/-}$ recipients (no significant difference; unpaired Student's *t*-test with Welch's correction; $P = 0.401$). Nuclei were counterstained with DAPI (*gray*, **A**, **B**, **C**, **D**). *Scale bars*: (**A**), (**B**) and (**D**): 10 μm; (**A1–A6**), (**B1–B3**), and (**D1–D3**): 5 μm; (**C–C4**): 20 μm. (**A1–A6**), (**B1–B3**), and (**D1–D3**): digital magnification of the *dashed square* in (**A**), (**B**), and (**D**), respectively. PSD-95, postsynaptic density protein 95.

Investigative Ophthalmology & Visual Science

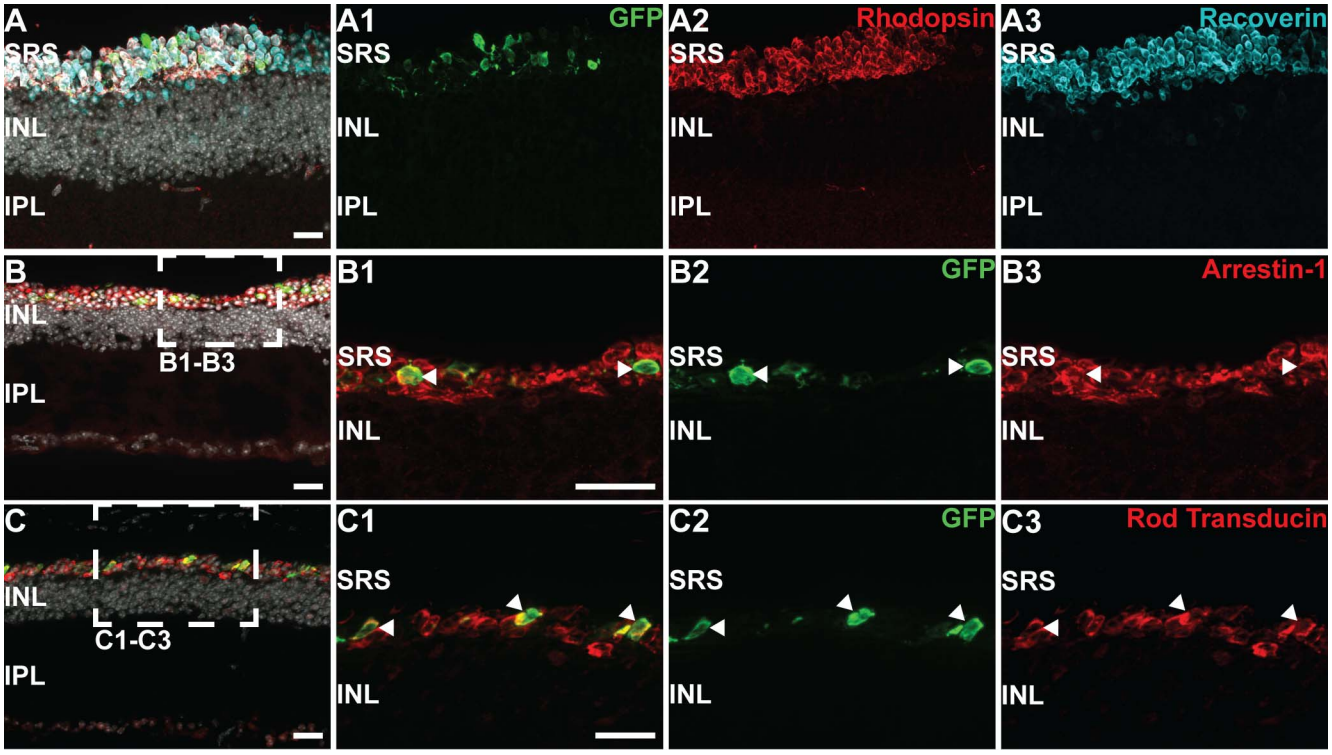

Figure 5. Transplanted mES-derived rods survive and express photo-transduction markers in the tg(Cpfl1;Rho$^{-/-}$) retina. (**A–C**) In complete ONL degenerated retinas of tg(Cpfl1;Rho$^{-/-}$) mice grafted rods (*green*, GFP) survive in the subretinal space for 4 weeks and express the photo-transduction markers rhodopsin (*red*, **A**, **A2**), recoverin (*cyan*, **A**, **A3**), arrestin-1 (*red*, **B**, **B1**, **B3**), and rod transducin (*red*, **C**, **C1**, **C3**). (**B1–B3**) and (**C1–C3**) are digital magnifications of the *dashed squares* in (**B**) and (**C**), respectively. Nuclei were counterstained with DAPI (*gray*, **A**, **B**, **C**). *Scale bars*: 20 μm. SRS, subretinal space.

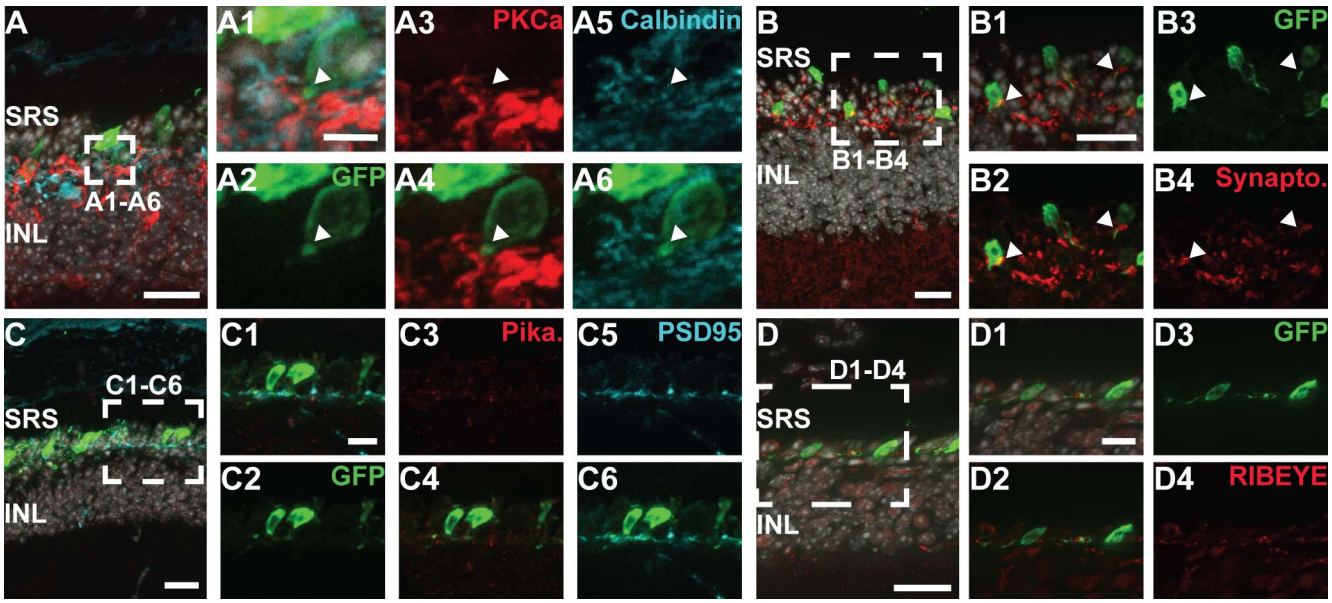

Figure 6. Synaptic marker expression in rod transplanted tg(Cpfl1;Rho$^{-/-}$) mice. Transplanted mES-derived rods (*green*, GFP) are localized in the SRS in close proximity to the host INL (**A–D**) with few axonal terminals of GFP^{+} donor cells in close contact to rod bipolar (PKCa^{+}, *red*) and horizontal (calbindin^{+}, *cyan*) cells (*arrowhead*, **A**, **A1–A6**). Dendrites of rod bipolar (PKCa^{+}, *red*) and horizontal (calbindin^{+}, *cyan*) cells show reduced ramification in tg(Cpfl1;Rho$^{-/-}$) hosts (**A**, **A1**, **A3–A6**; compare with Figure S4A, wild-type). Some grafted mES-derived rods express the synaptic markers synaptophysin (*red*, **B**, **B1**, **B3**, **B4**) and PSD-95 (*cyan*, **C**, **C1**, **C5**, **C6**), whereas pikachurin (*red*, **C**, **C1**, **C3**, **C4**) and RIBEYE (*red*, **D**, **D1**, **D2**, **D4**) are expressed in low amounts or are not detectable. *Scale bars*: (**A**), (**B**), (**B1–B4**), (**C**), and (**D**): 20 μm; (**A1–A6**): 5 μm; (**C1–C6**) and (**D1–D4**): 10 μm. (**A1–A6**), (**B1–B4**), (**C1–C6**), and (**D1–D4**) are a digital magnification of the *dashed square* in (**A**), (**B**), (**C**), and (**D**), respectively. In (**A**), (**B**), (**B1**), (**C**), (**D**), and (**D1**), nuclei were stained with DAPI (*gray*).

Investigative Ophthalmology & Visual Science

observations in wild-type hosts. Integrated rods acquired a mature morphology, expressed pan- and rod-specific photoreceptor as well as several synaptic markers, and presented striking similarities with endogenous rod photoreceptors.

Conversely, our data in the tg(Cpfl1;Rho$^{-/-}$) model with rapid cone-rod loss suggest that donor photoreceptor integration and morphology might be highly dependent on the host environment. Notably, in our newly established tg(Cpfl1;Rho$^{-/-}$) mouse model with complete photoreceptor loss, grafted rods survived in the subretinal space. However, transplanted cells did not show distinctive mature photoreceptor morphologic features, such as the presence of outer segments and synaptic terminals. Despite the expression of several photo-transduction markers (i.e., recoverin, rhodopsin, arrestin-1, and rod transducin), several synaptic markers were incompletely expressed in tg(Cpfl1;Rho$^{-/-}$) hosts grafted with rods. Particularly, the synapse adaptor protein pikachurin and the ribbon synapse marker RIBEYE were expressed at very low levels or were undetectable and dendrites of rod bipolars were atrophic in tg(Cpfl1;Rho$^{-/-}$) mice with very few points of contact observed between GFP^{+} donor cells and endogenous second-order neurons. The absence of key synaptic markers suggests insufficiently established synapses between donor and host cells. Additionally, we did not observe restoration of the dendritic arborization of rod bipolars and horizontals in transplanted tg(Cpfl1;Rho$^{-/-}$) mice, which might contribute to the absence of presynaptic markers. This raises the question of whether a remaining ONL, like in the Prom1$^{-/-}$ model, is necessary for donor cell integration, (e.g., host photoreceptors and Müller glia processes might act as a scaffold for migrating cells, also allowing the formation of proper synaptic connections). Thus, it might be necessary to develop strategies to promote synapse formation, like addition of brain-derived neurotrophic factor (BDNF)[49] and chondroitinase ABC[50] or to induce dendrite growth/arborization with BDNF or Down Syndrome Cell Adhesion Molecule.[51–53]

Additional factors in tg(Cpfl1;Rho$^{-/-}$) mice beside the complete loss of photoreceptors might have influenced donor photoreceptor morphology, integration, and connectivity. Severely degenerated retinas represent a hostile environment often combined with reactive gliosis, immune responses, and dendritic remodeling. This might result in the formation of a barrier to grafted cells inhibiting integration and extension of synapses to second-order neurons, thus explaining the improper expression of synaptic markers. Additionally, although the eye is considered to be immune-privileged, complete photoreceptor loss might result in activated microglia and increased immune cell invasion that influence donor photoreceptors. Thus, transplantation at earlier time points into tg(Cpfl1;Rho$^{-/-}$) mice before total photoreceptor degeneration occurs, would help to identify and dissect factors that influence donor cell morphology, integration, and synapse formation.

Full-field ERG measurements showed no functional improvements in transplanted tg(Cpfl1;Rho$^{-/-}$) mice. However, potential functional repair has to be analyzed in further studies using more sensitive technologies given that approximately 150,000 properly connected photoreceptors are necessary to receive robust ERG answers.[15] The number of 200,000 transplanted donor photoreceptors with expected significant cell loss due to the injection procedure might be too low for gaining visual improvements measurable by ERG. Thus, besides improving synapse formation also grafting of increased numbers of donor photoreceptors should be considered in future photoreceptor replacement studies.

Most photoreceptor transplantation studies performed so far approached recipients with an ONL present,[7,14,15,23,25] like the Prom1$^{-/-}$ mice, whereas mouse models with a completely degenerated ONL were rarely used.[12,40] A recent study provided evidence for some functional recovery following transplantation of primary rod photoreceptors into another mouse model of rapid and complete photoreceptor loss: the rd1 mouse.[12] However, a detailed analysis of synaptic marker expression beside synaptophysin has not been performed in this study. Furthermore, another report suggested additional functional impairment in the rd1 strain C3H/HeN by a second mutation in Gpr179, a G-protein–coupled receptor localized to dendrites of ON-bipolar cells,[54] thus questioning the mechanisms by which rod transplantation might have resulted in functional repair in this retinal degeneration model.

In conclusion, we provide evidence for the efficient generation of transplantable rod photoreceptors from an expandable and scalable cell source. The in vitro differentiation of mES-derived rods combined with single cell-surface marker MACS enrichment represents a potential future strategy for clinical grade photoreceptor production for transplantation. Differential engraftment of mES-derived rods into mouse models of retinal degeneration reveals the importance of the host disease state, type, and environment for photoreceptor integration, maturation, and synapse formation. Thus, further studies of donor photoreceptor connectivity to the host retinal circuitry within animal models of severe retinal degeneration might be crucial to develop photoreceptor replacement approaches toward clinical application. The herein established double-mutant mouse model will serve as a potential benchmark model for preclinical studies of transplantable photoreceptors generated from pluripotent stem cells to evaluate their use for replacement therapies in the retina.

Acknowledgments

We thank Elisabeth Schulze, Susanne Kretschmar, and Kerstin Skokann for technical support; Sindy Böhme, Emily Lessmann, and Katrin Baumgart for animal husbandry; Wieland Huttner and Anne-Marie Marzesco for providing prominin1 KO mice; Pete Humphries and Jane Farrar for providing Rho$^{-/-}$ mice; and Bernd Wissinger and Bo Chang for Cpfl1 mice.

Supported by the Deutsche Forschungsgemeinschaft (DFG) FZT 111 Center for Regenerative Therapies Dresden, Cluster of Excellence (MA and MOK), DFG Grant AD375/3-1 (MA), DZNE Helmholtz (MOK), the Fundação para a Ciência e a Tecnologia (FCT: SFRH/BD/60787/2009; TS-F), Center for Integrated Protein Science Munich CiPSM, Cluster of Excellence EXC114 (SM). Longterm structural funding from Methusalem Funding by the Flemish Government (PC).

Disclosure: **T. Santos-Ferreira**, None; **M. Völkner**, None; **O. Borsch**, None; **J. Haas**, None; **P. Cimalla**, None; **P. Vasudevan**, None; **P. Carmeliet**, None; **D. Corbeil**, None; **S. Michalakis**, None; **E. Koch**, None; **M.O. Karl**, None; **M. Ader**, None

References

1. Prokofyeva E, Zrenner E. Epidemiology of major eye diseases leading to blindness in Europe: a literature review. *Ophthalmic Res*. 2012;47:171–188.
2. Acland GM, Aguirre GD, Ray J, et al. Gene therapy restores vision in a canine model of childhood blindness. *Nat Genet*. 2001;28:92–95.
3. Maeda T, Maeda A, Casadesus G, Palczewski K, Margaron P. Evaluation of 9-cis-retinyl acetate therapy in Rpe65−/− mice. *Invest Ophthalmol Vis Sci*. 2009;50:4368–4378.

4. Busskamp V, Duebel J, Balya D, et al. Genetic reactivation of cone photoreceptors restores visual responses in retinitis pigmentosa. *Science*. 2010;329:413–417.
5. D Trifunović AS. Neuroprotective strategies for the treatment of inherited photoreceptor degeneration. *Curr Mol Med*. 2012;12:598–612.
6. Schön C, Biel M, Michalakis S. Retinal gene delivery by adeno-associated virus (AAV) vectors: strategies and applications. *Eur J Pharm Biopharm*. 2015;95:343–352.
7. MacLaren RE, Pearson RA, MacNeil A, et al. Retinal repair by transplantation of photoreceptor precursors. *Nature*. 2006; 444:203–207.
8. Bartsch U, Oriyakhel W, Kenna PF, et al. Retinal cells integrate into the outer nuclear layer and differentiate into mature photoreceptors after subretinal transplantation into adult mice. *Exp Eye Res*. 2008;86:691–700.
9. Eberle D, Schubert S, Postel K, Corbeil D, Ader M. Increased integration of transplanted CD73-positive photoreceptor precursors into adult mouse retina. *Invest Ophthalmol Vis Sci*. 2011;52:6462–6471.
10. Barber AC, Hippert C, Duran Y, et al. Repair of the degenerate retina by photoreceptor transplantation. *Proc Natl Acad Sci U S A*. 2013;110:354–359.
11. Lakowski J, Han Y-T, Pearson RA, et al. Effective transplantation of photoreceptor precursor cells selected via cell surface antigen expression. *Stem Cells*. 2011;29:1391–1404.
12. Singh MS, Issa PC, Butler R, et al. Reversal of end-stage retinal degeneration and restoration of visual function by photoreceptor transplantation. *Proc Natl Acad Sci U S A*. 2013;110: 1101–1106.
13. Eberle D, Santos-Ferreira T, Grahl S, Ader M. Subretinal transplantation of MACS purified photoreceptor precursor cells into the adult mouse retina. *J Vis Exp*. 2014;84:e50932.
14. Warre-Cornish K, Barber AC, Sowden JC, Ali RR, Pearson RA. Migration, integration and maturation of photoreceptor precursors following transplantation in the mouse retina. *Stem Cells Dev*. 2013;23:941–954.
15. Pearson RA, Barber AC, Rizzi M, et al. Restoration of vision after transplantation of photoreceptors. *Nature*. 2012;485:99–103.
16. Santos-Ferreira T, Postel K, Stutzki H, Kurth T, Zeck G, Ader M. Daylight vision repair by cell transplantation. *Stem Cells*. 2015; 33:79–90.
17. Eiraku M, Takata N, Ishibashi H, et al. Self-organizing optic-cup morphogenesis in three-dimensional culture. *Nature*. 2011; 472:51–56.
18. Nakano T, Ando S, Takata N, et al. Self-formation of optic cups and storable stratified neural retina from human ESCs. *Cell Stem Cell*. 2012;10:771–785.
19. Osakada F, Ikeda H, Sasai Y, Takahashi M. Stepwise differentiation of pluripotent stem cells into retinal cells. *Nat Protoc*. 2009;4:811–824.
20. Osakada F, Ikeda H, Mandai M, et al. Toward the generation of rod and cone photoreceptors from mouse, monkey and human embryonic stem cells. *Nat Biotechnol*. 2008;26:215–224.
21. Ohlemacher SK, Iglesias CL, Sridhar A, Gamm DM, Meyer JS. Generation of highly enriched populations of optic vesicle—like retinal cells from human pluripotent stem cells. 2007. Available at: http://onlinelibrary.wiley.com/doi/10.1002/9780470151808.sc01h08s32/abstract. Accessed June 19, 2015.
22. Lamba DA, Karl MO, Ware CB, Reh TA. Efficient generation of retinal progenitor cells from human embryonic stem cells. *Proc Natl Acad Sci U S A*. 2006;103:12769–12774.
23. Gonzalez-Cordero A, West EL, Pearson RA, et al. Photoreceptor precursors derived from three-dimensional embryonic stem cell cultures integrate and mature within adult degenerate retina. *Nat Biotechnol*. 2013;31:741–747.
24. Boucherie C, Mukherjee S, Henckaerts E, Thrasher AJ, Sowden JC, Ali RR. Brief report: self-organizing neuroepithelium from human pluripotent stem cells facilitates derivation of photoreceptors. *Stem Cells*. 2013;31:408–414.
25. Decembrini S, Koch U, Radtke F, Moulin A, Arsenijevic Y. Derivation of traceable and transplantable photoreceptors from mouse embryonic stem cells. *Stem Cell Rep*. 2014;2:853–865.
26. Zacchigna S, Oh H, Wilsch-Bräuninger M, et al. Loss of the cholesterol-binding protein prominin-1/CD133 causes disk dysmorphogenesis and photoreceptor degeneration. *J Neurosci*. 2009;29:2297–2308.
27. Chang B, Hawes NL, Hurd RE, Davisson MT, Nusinowitz S, Heckenlively JR. Retinal degeneration mutants in the mouse. *Vision Res*. 2002;42:517–525.
28. Humphries MM, Rancourt D, Farrar GJ, et al. Retinopathy induced in mice by targeted disruption of the rhodopsin gene. *Nat Genet*. 1997;15:216–219.
29. Koch S, Sothilingam V, Garcia Garrido M, et al. Gene therapy restores vision and delays degeneration in the CNGB1(–/–) mouse model of retinitis pigmentosa. *Hum Mol Genet*. 2012; 21:4486–4496.
30. D'Costa S, Blouin V, Broucque F, et al. Practical utilization of recombinant AAV vector reference standards: focus on vector genomes titration by free ITR qPCR. *Mol Ther Methods Clin Dev*. 2016;5:16019.
31. Michalakis S, Mühlfriedel R, Tanimoto N, et al. Restoration of cone vision in the CNGA3–/– mouse model of congenital complete lack of cone photoreceptor function. *Mol Ther J Am Soc Gene Ther*. 2010;18:2057–2063.
32. Li J-Y, Christophersen NS, Hall V, Soulet D, Brundin P. Critical issues of clinical human embryonic stem cell therapy for brain repair. *Trends Neurosci*. 2008;31:146–153.
33. Tucker BA, Park I-H, Qi SD, et al. Transplantation of adult mouse iPS cell-derived photoreceptor precursors restores retinal structure and function in degenerative mice. *PLoS One*. 2011;6:e18992.
34. Lamba DA, Gust J, Reh TA. Transplantation of human embryonic stem cell-derived photoreceptors restores some visual function in Crx-deficient mice. *Cell Stem Cell*. 2009;4: 73–79.
35. Spiwoks-Becker I, Vollrath L, Seeliger MW, Jaissle G, Eshkind LG, Leube RE. Synaptic vesicle alterations in rod photoreceptors of synaptophysin-deficient mice. *Neuroscience*. 2001;107: 127–142.
36. Aartsen WM, Kantardzhieva A, Klooster J, et al. Mpp4 recruits Psd95 and Veli3 towards the photoreceptor synapse. *Hum Mol Genet*. 2006;15:1291–1302.
37. Regus-Leidig H, tom Dieck S, Brandstätter JH. Absence of functional active zone protein Bassoon affects assembly and transport of ribbon precursors during early steps of photoreceptor synaptogenesis. *Eur J Cell Biol*. 2010;89:468–475.
38. Sato S, Omori Y, Katoh K, et al. Pikachurin, a dystroglycan ligand, is essential for photoreceptor ribbon synapse formation. *Nat Neurosci*. 2008;11:923–931.
39. Yang Z, Chen Y, Lillo C, et al. Mutant prominin 1 found in patients with macular degeneration disrupts photoreceptor disk morphogenesis in mice. *J Clin Invest*. 2008;118:2908–2916.
40. Eberle D, Kurth T, Santos-Ferreira T, Wilson J, Corbeil D, Ader M. Outer segment formation of transplanted photoreceptor precursor cells. *PLoS One*. 2012;7:e46305.
41. Meyer JS, Howden SE, Wallace KA, et al. Optic vesicle-like structures derived from human pluripotent stem cells facilitate a customized approach to retinal disease treatment. *Stem Cells*. 2011;29:1206–1218.

42. Reichman S, Terray A, Slembrouck A, et al. From confluent human iPS cells to self-forming neural retina and retinal pigmented epithelium. *Proc Natl Acad Sci U S A*. 2014;111:8518–8523.
43. Zhong X, Gutierrez C, Xue T, et al. Generation of three-dimensional retinal tissue with functional photoreceptors from human iPSCs. *Nat Commun*. 2014;5:4047.
44. Koso H, Minami C, Tabata Y, et al. CD73, a novel cell surface antigen that characterizes retinal photoreceptor precursor cells. *Invest Ophthalmol Vis Sci*. 2009;50:5411–5418.
45. Lakowski J, Gonzalez-Cordero A, West EL, et al. Transplantation of photoreceptor precursors isolated via a cell surface biomarker panel from embryonic stem cell-derived selfforming retina. *Stem Cells*. 2015;33:2469–2482.
46. Richel DJ, Johnsen HE, Canon J, et al. Highly purified CD34+ cells isolated using magnetically activated cell selection provide rapid engraftment following high-dose chemotherapy in breast cancer patients. *Bone Marrow Transplant*. 2000;25:243–249.
47. Handgretinger R, Lang P, Schumm M, et al. Isolation and transplantation of autologous peripheral CD34+ progenitor cells highly purified by magnetic-activated cell sorting. *Bone Marrow Transplant*. 1998;21:987–993.
48. Chou T, Sano M, Ogura M, Morishima Y, Itagaki H, Tokuda Y. Isolation and transplantation of highly purified autologous peripheral CD34$^+$ progenitor cells: purging efficacy, hematopoietic reconstitution following high dose chemotherapy in patients with breast cancer: results of a feasibility study in Japan. *Breast Cancer*. 2005;12:178–188.
49. Sanchez AL, Matthews BJ, Meynard MM, Hu B, Javed S, Cohen-Cory S. BDNF increases synapse density in dendrites of developing tectal neurons in vivo. *Development*. 2006;133:2477–2486.
50. Suzuki T, Akimoto M, Imai H, et al. Chondroitinase ABC treatment enhances synaptogenesis between transplant and host neurons in model of retinal degeneration. *Cell Transplant*. 2007;16:493–503.
51. Lom B, Cohen-Cory S. Brain-derived neurotrophic factor differentially regulates retinal ganglion cell dendritic and axonal arborization in vivo. *J Neurosci*. 1999;19:9928–9938.
52. Fuerst PG, Koizumi A, Masland RH, Burgess RW. Neurite arborization and mosaic spacing in the mouse retina require DSCAM. *Nature*. 2008;451:470–474.
53. Lazo OM, Gonzalez A, Ascaño M, Kuruvilla R, Couve A, Bronfman FC. BDNF regulates Rab11-mediated recycling endosome dynamics to induce dendritic branching. *J Neurosci*. 2013;33:6112–6122.
54. Nishiguchi KM, Carvalho LS, Rizzi M, et al. Gene therapy restores vision in rd1 mice after removal of a confounding mutation in Gpr179. *Nat Commun*. 2015;6:6006.

Investigative Ophthalmology & Visual Science